Analysis on Efficacy of Chitosan-Based Gel on Bone Quality and Quantity

Soher Nagi Jayash[1,2]*, Najihah Mohd Hashim[3], Misni Misran[4], Norliza Ibrahim[5], Nisreen Mohammed AL-Namnam[6] and N. A. Baharuddin[2]*

[1]School of Dentistry, University of Birmingham, Birmingham, United Kingdom, [2]Department of Restorative Dentistry, Faculty of Dentistry, University of Malaya, Kuala Lumpur, Malaysia, [3]Department of Pharmacy, Faculty of Medicine, University of Malaya, Kuala Lumpur, Malaysia, [4]Department of Chemistry, Faculty of Science, University of Malaya, Kuala Lumpur, Malaysia, [5]Department of Oral & Maxillofacial Clinical Sciences, Faculty of Dentistry, University of Malaya, Kuala Lumpur, Malaysia, [6]Department of Oral Surgery, Faculty of Dentistry, University of Sana'a, Sana'a, Yemen

Objectives: To assess and compare the quantity and the quality of the newly bone generated when using chitosan-based gel scaffold and osteoprotegerin-chitosan gel scaffold.

Methods: A total of 18 critical-sized defects on New Zealand white rabbit craniums were created. In 12 defects, either chitosan gel or osteoprotegerin-chitosan gel was implanted the last six defects were kept unfilled as a control. Bone formation was examined at 6 and 12 weeks. Bone's specimens were scanned using the High-resolution peripheral quantitative computed tomography. Histological and histomorphometric analysis were carried out to compare the volume and area of regenerated bone.

Results: The results of the HR-pQCT showed that bone volume and densities in the osteoprotegerin-chitosan gel group were significantly higher than the chitosan gel and control groups whereas, the bone volume density in the chitosan gel group was significantly higher than the control group in both intervals time ($p = 0.01$, $p = 000$). No significant difference in bone volume between the chitosan gel and control groups ($p = 0.506$, $p = 0.640$) was observed. However, similar findings were shown in the histomorphometric analysis, with the highest new bone formation was observed in the OPG-chitosan gel group followed by the chitosan group. The mean percentage of new bone was greater at 12 weeks compared to 6 weeks in all groups.

Conclusions: Chitosan-based gel demonstrated a significant bone quantity and quality compared to unfilled surgical defects. Consistently, osteoprotegerin enhanced the chitosan gel in bone regeneration.

Keywords: bone regeneration, chitosan, HR-pQCT, histomorphometry, osteoprotegerin

INTRODUCTION

Hydrogels are attractive materials because of their carrier ability of proteins, growth factors, cells, and other necessary components for tissue engineering. Successfully, injectable hydrogels systems can be used in minimally invasive surgical applications and utilized for encapsulating a variety of different biological materials such as cells, growth factors, and drugs. In addition, they can form gels capable of filling any target area of any shape following their injection (Lee, 2018; Al-Namnam and Jayash, 2019; Sharma and Sharma, 2020).

Chitosan is a natural polysaccharide copolymer which is widely used in drug delivery and bone tissue regeneration. It was reported that chitosan exhibits osteoconductive and enhanced wound healing properties, which suggested that chitosan may be useful as a bioactive coating to improve the ossification of orthopaedic and craniofacial implants (Bumgardner et al., 2003; Malviya, 2020). Combination of Chitosan with different bio-active material supports its activity in bone healing. Chitosan-γPGA polyelectrolyte complex hydrogel (C-PGA) has been developed and showed to be effective in new bone formation in the alveolar socket following tooth extraction (Chang et al., 2014). Furthermore. Combination of OPG with chitosan (OPG-chitosan matrices) in enhancing cell growth and proliferation, and in inducing the production of osteopontin and osteocalcin protein levels has been established (Jayash et al., 2016).

The technology in bone structure investigation has always been limited to a two-dimensional histological method. A microcomputed tomography (μCT) scanner allows a three-dimensional (3D) evaluation of histological specimens. Moreover, it's a rapid non-destructive process and an objective standardized approach of bone evaluation. This automated analysis method is much faster than any manual procedures (Baiker et al., 2012; Particelli et al., 2012). Good correlation between bone structural measures obtained from microcomputed tomography (μCT) datasets and from histological sections confirms that μCT may be an efficient tool for the characterization of bone structure (Particelli et al., 2012). Studies have confirmed that the High-resolution peripheral quantitative computed tomography (HR-pQCT) scanner, one type of μCT method, is a useful and reliable method for evaluating bone healing (Maréchal et al., 2005; Acar et al., 2016).

Micro-computed tomography (Micro-CT) images can be used to quantitatively represent bone geometry through a range of computed attenuation-based parameters. Xtreme CT (high-resolution peripheral quantitative computed tomography, HR-pQCT) is a new technology that uses the same principles as Micro-CT but can achieve a much higher spatial resolution and still has a very low radiation dose. It is able to define bones surfaces in a three-dimensional manner, and provides information on bone microarchitecture as well as bone density. Thus, this study aimed to investigate the osteogenic ability of chitosan-based gel in critical size defects on rabbits by evaluating the morphological feature, quantity and quality of the new bone that formed within chitosan-based gels compared to normal bone healing at several points in time using HR-pQCT and histomorphometric analysis.

MATERIALS AND METHODS

Chitosan-Based Gel and OPG Chitosan Gel Preparation

Two sets of water-soluble chitosan (25 kDa) gels were prepared by dissolving 50 mg of water-soluble chitosan in Tris buffer (5 mmol L^{-1}, pH 7.5). The mixtures were then left overnight to allow chitosan to completely dissolve. For one set of the gels, 1 mg ml^{-1} recombinant human OPG protein (Recombinant Human OPG, PeproTech, Rocky Hill, New Jersey, United States) was added. The other set was left without any addition of recombinant human OPG protein. Chitosan binder (85 kDa) was added to all the gel formulations. They were then mixed and allowed it to stand overnight under vacuum at room temperature (25°C). The gels were later sterilized by gamma radiation (4 kGy) and kept in desiccators (Jayash et al., 2017a).

Experimental Animals

The animal experiment was authorized according to the Institutional Animal Care and Use Committee. A total of 18 New Zealand white female rabbits (6 months old, 3.5–45–4 kg) were divided randomly into three groups of six; left unfilled (control) (group A), chitosan gel (group B), OPG-chitosan gel (group C). Three rabbits from each group were located randomly to be sacrificed at following time point: 6 and 12 months.

For the surgical procedures, the rabbits were anaesthetized with 30 mg/kg of ketamine 100 mg/ml and 3 mg/kg of xylazine 20 mg/ml (Troy laboratories PTY. Limited, Smithfield, Australia). Following hair shaving and disinfection of the operation site, full thickness a cranial critical size defect of 15 mm in diameter was created. After the placement of test materials or control, the defects were closed layer-by-layer. Bone formation was examined at 6 and 12 weeks time points, where three rabbits from each group were sacrificed at 6 and 12 weeks after surgery.

Animal Euthanasia

After anesthesia was induced by usual means, the rabbit was euthanized by using cardiac puncture with an overdose of barbiturates (Dolethal, Pentobarbitone sodium 200 mg ml^{-1} solution, 0.7 ml kg^{-1} IV) according to the assigned time points either 6 and 12 weeks.

HR-pQCT Evaluation

The region of interest in the bone specimens was scanned using the HR-pQCT (XtremeCT, Scanco Medical AG, Switzerland) with an isotropic voxel size of 82 μm and scanning area length of 25 mm. Each scan consists of 154 parallel CT slices. The 3D construction of surgical area, bone volume, and bone density were measured by using the XtremeCT software, Materialise Mimics Innovation Suite 17.0, Materialise 3-matic® Medical 9.0 and SkyScan "CT-analyser" software (version 1.1).

Rabbit's native parietal bone (15 × 15 mm dimension) was scanned and used as a reference. All the surgical sites were

TABLE 1 | Comparison of means bone volume and bone volume density between groups (group A (control), group B (chitosan gel), group C (OPG-chitosan gel)).

	Bone volume (mm^3)			Bone volume density%		
	6 weeks	12 weeks	p value	6 weeks	12 weeks	p value[b]
Group A	189 ± 36	267 ± 55	$p \geq 0.05$	21 ± 3.2	61 ± 6[b]	$p \leq 0.05$
Group B	256 ± 51	385 ± 30[ab]	$p \leq 0.05$	45 ± 5[a]	77 ± 7[ab]	$p \leq 0.05$
Group C	353 ± 50[a]	537 ± 55[ab]	$p \leq 0.05$	71 ± 1[a]	88 ± 2[ab]	$p \leq 0.05$
p value[a]	$p \leq 0.05$	$p \leq 0.05$		$p \leq 0.05$	$p \leq 0.05$	

[a]indicates between groups significant difference over time based on One-Way ANOVA (p ≤ 0.05).
[b]indicates between groups significant difference over time based on independent-samples t-test (p < 0.05).

scanned at 6 and 12 weeks after surgeries. The Scanco XtremeCT device allowed the following evaluations of the healing surgical defects: 1) a 3D model color map comparison, 2) Mean bone volume and bone volume density comparison, and 3) Tissue density comparison (periphery and centre of the surgical defects). The 3D model colour map was constructed by superimposing the scanned images of the reference bone and the newly formed tissue at the surgical sites after surgery. The differences between them were shown as colour coding where green indicates no change between them, yellow indicates some change and red indicates a great difference. All measurements were analyzed using the Materialise Mimics Innovation Suite 17.0, Materialise 3-matic® Medical 9.0 and SkyScan "CT-analyser" software.

Histomorphometric Analysis

Upon completion of the experimental periods for each group, the animals were sacrificed, and the parietal bones from each rabbit were dissected and subjected to conventional decalcification, embedding, sectioning and hematoxylin and eosin staining (Jayash et al., 2017a). Histology specimens were digitized using the panoramic scan digital slide scanner (3DHISTECH, Budapest, Hungary). Subsequently, the histological images were assessed using the panoramic viewer software version 1.15.3 (3DHISTECH, Budapest, Hungary) at 200 scale bars. The Image-Pro Express software (Media Cybernetics Inc., Bethesda, MD, United States) was used for quantitative analysis. A 48-point grid of each image was overlaid to measure the amount of newly formed bone, osteoid tissue, bone marrow and fibrous tissue using the point-counting method. The amount of new bone formation, osteoid tissue, bone marrow and fibrous tissue was calculated as the percentage of new bone and graft area to the total defect area (Alyessary et al., 2017). Inter-examiner reliability for measuring methods was assessed by two blinded examiners. Reliability was evaluated using the Cronbach alpha test.

Statistical Analysis

Statistical analysis was performed using parametric One-way ANOVA test to compare the mean values of the bone volume, bone volume density and mean percentages of newly formed tissue between the groups (group A (control), group B (chitosan gel), group C (OPG-chitosan gel)). The groups were compared with Tukey's post-hoc test in case of a significant result. The significance value was set at ($p < 0.05$). Values were presented as a mean (arithmetic mean) and standard deviation.

RESULTS

Bone Volume and Bone Volume Density Results

Table 1 summarizes the means and standard deviations of bone volume (mm^3) and mean percentages of bone volume density for all groups over different time points. In intragroup comparison of the mean bone volume in the different group, it showed a highly significant mean bone volume at 12 weeks compared to 6 weeks ($p = 0.000$, $p = 0.001$) in OPG-chitosan gel group and chitosan gel group. However, no significant difference showed in control group at both interval time ($p = 0.16$). In intergroup comparison, it showed that chitosan gel group had a significantly higher mean bone volume compared to control group and chitosan gel group at both time points ($p = 0.000$). Additionally, no significant difference has been revealed in the mean bone volume between control group and chitosan gel group at week 6 after surgery ($p = 0.109$). Whereas, a significant mean difference was observed in the bone volume of control group compared to chitosan gel group at 12 weeks ($p = 0.001$) (**Figure 1**).

The intragroup comparison of bone volume densities in the different groups showed a significant difference in the mean bone volume density at 6 weeks compared to 12 weeks
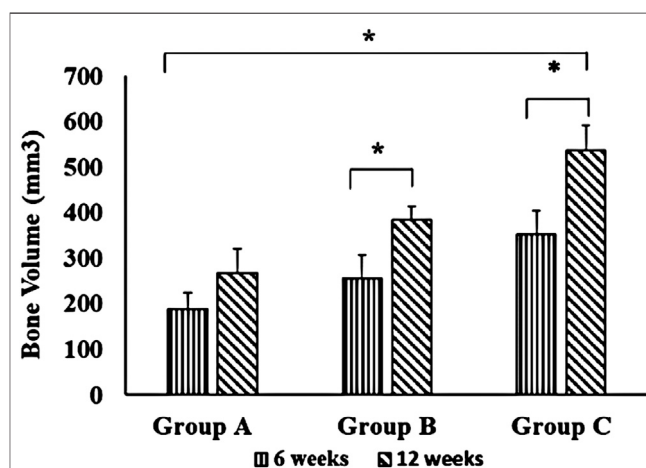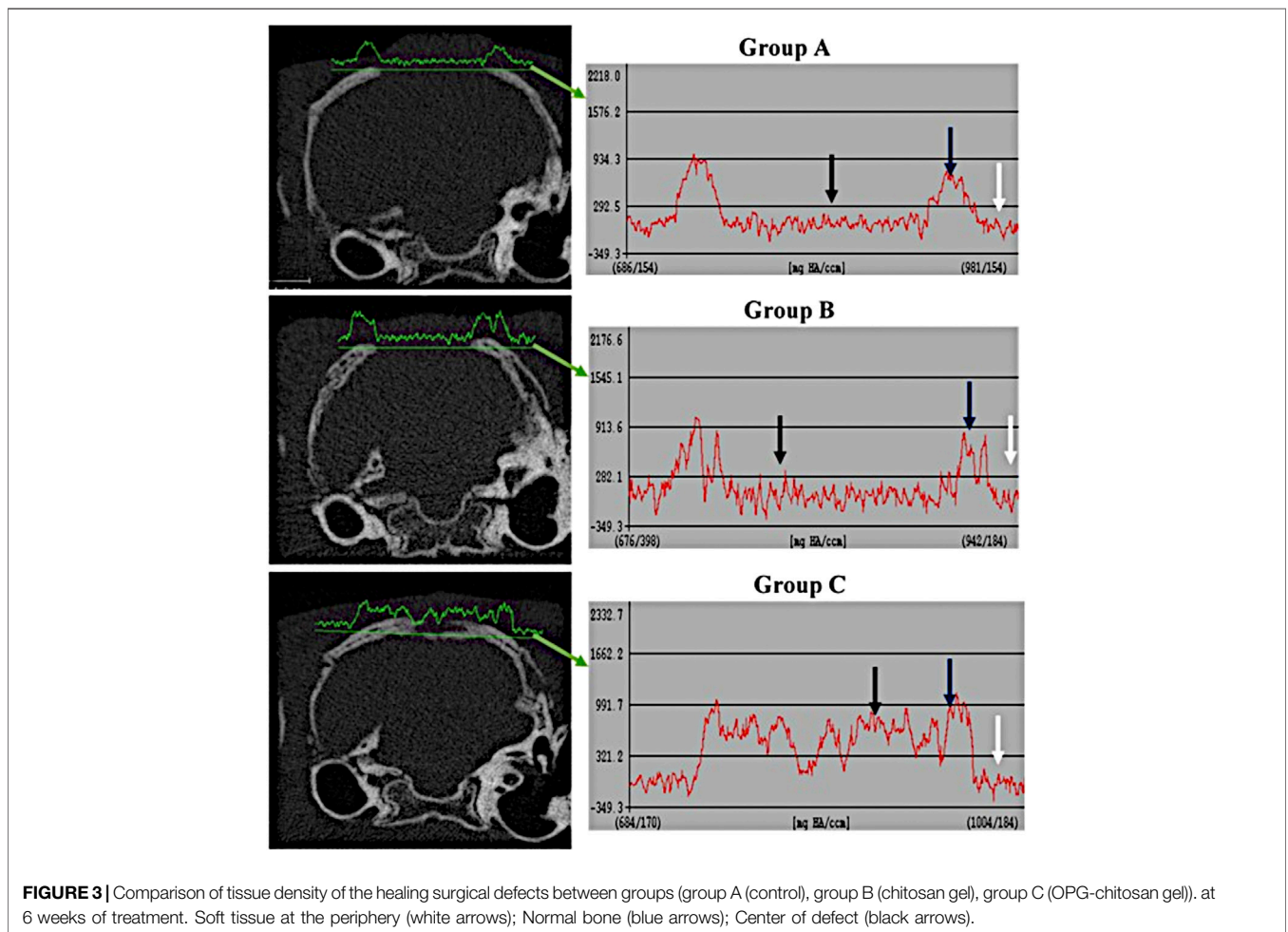

FIGURE 1 | Comparison of bone volume between groups (group A (control), group B (chitosan gel), group C (OPG-chitosan gel). at 6 and 12 weeks. Data are expressed as mean ± SD ($n = 3$). *denotes significant difference in bone volume ($p < 0.05$) found between different groups.

FIGURE 2 | Comparison of bone volume densities between groups (group A (control), group B (chitosan gel), group C (OPG-chitosan gel)). at 6 and 12 weeks. Data are expressed as mean ± SD (n = 3). *denotes significant difference in bone volume (p < 0.05) found between different groups.
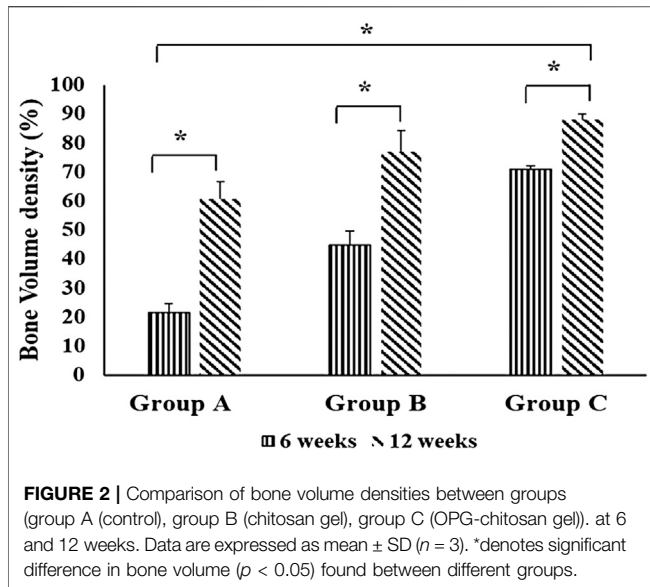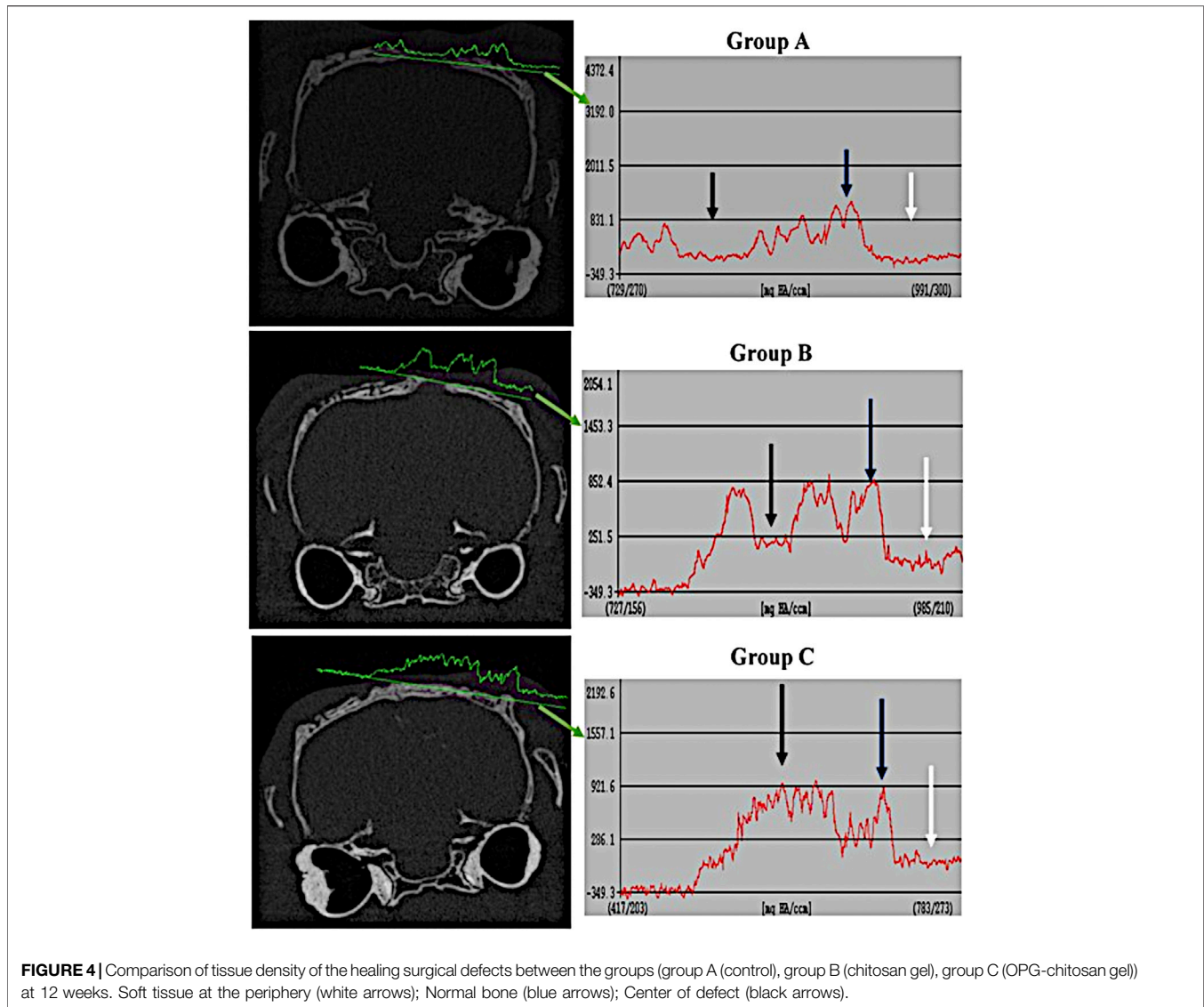
in all groups. In the intergroup comparison, it revealed a highly significant bone volume density at 6 and 12 weeks in group C compared to control group and chitosan gel group (p = 0.000). Bone volume density in chitosan gel group was significantly higher than control group at 6 and 12 weeks (**Figure 2**).

Comparison of Tissue Density at the Periphery and Center of the Healing Surgical Defects

The comparison of tissue density at the periphery and center of the defect between the different groups are shown in **Figures 3**, **4**. It revealed that the density of tissue at the center and native soft tissue at the periphery of the defect was comparable in group A (unfilled defect; control group) at both interval time (6 and 12 weeks). Whereas, it exposed an increase at the center of the defect compared to the native soft tissue at the periphery in chitosan gel filled defects (group B) although this increasing was

FIGURE 3 | Comparison of tissue density of the healing surgical defects between groups (group A (control), group B (chitosan gel), group C (OPG-chitosan gel)). at 6 weeks of treatment. Soft tissue at the periphery (white arrows); Normal bone (blue arrows); Center of defect (black arrows).

FIGURE 4 | Comparison of tissue density of the healing surgical defects between the groups (group A (control), group B (chitosan gel), group C (OPG-chitosan gel)) at 12 weeks. Soft tissue at the periphery (white arrows); Normal bone (blue arrows); Center of defect (black arrows).

lower than the density of the reference bone at both interval time. In OPG-chitosan gel filled defects (group C), the density of tissue in the center was markedly higher than the density of native soft tissue at the periphery at both interval time which revealed nearly comparable to the density of the reference bone at 12 weeks.

3D Models of Treated Groups

The construction of a 3D model of the surgical area of the different groups at 6 and 12 weeks post-surgery is shown in **Figure 5**. It exhibited the bone formation commenced along the margin of the defect progressing centrally where all the groups showed evidence of varying increasing in bone defect closure from 6 to 12 weeks post-surgery.
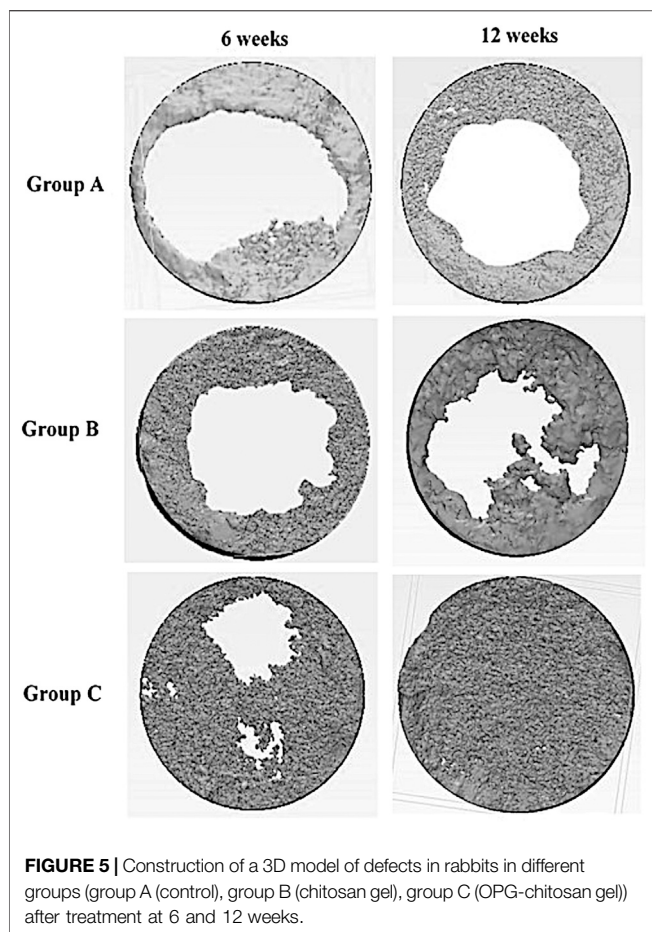
In the control and chitosan gel groups, the defects were not completely filled by the bone. It showed a discontinuous bone tissue layers centrally although it was continuous at the margin at both time interval time which covered the superficial portions of the defects partially. Even though, chitosan gel group displayed more bone tissue than control group group at both interval time. While the defects closure was more prominent in OPG-chitosan gel group compared to the others groups at 6 and 12 where it showed complete surgical bone defect closure at 12 weeks.

Part Comparison Color Map Results

Figure 6 shows the construction of a 3D model of the surgical areas of different groups at 6 and 12 weeks post-surgery. It was observed that the bone formation began along the margin of the defect toward the centre. The groups showed variation in the defect closure at 6 and 12 weeks post-surgery.

At 6 weeks post-surgery, the newly formed bone was more prominent in OPG-chitosan gel group where it covered most of the surgical defect compare to chitosan gel and control groups. At 12 weeks, control and chitosan gel groups showed partial defect closure, with more defects closing in chitosan gel group than control group, while OPG-chitosan gel group exhibited complete surgical bone defect closure.

FIGURE 5 | Construction of a 3D model of defects in rabbits in different groups (group A (control), group B (chitosan gel), group C (OPG-chitosan gel)) after treatment at 6 and 12 weeks.

In comparison to the reference bone, control group showed the most major differences in the bone tissues (green colour) covering the surgical defects at 6 and 12 weeks. However, it showed more bone formation at the periphery of defects at 12 weeks compared to that observed at 6 weeks. More bone formation and less soft tissue (red colour) was observed in chitosan gel group than that in control group in comparison to the reference bone at both time points. Remarkably, OPG-chitosan gel group showed comparable bone formation to the reference bone at both interval times, where green colour was noticed covering all the surface area of the defect.

Histomorphometric Analysis

In terms of intragroup comparison, histomorphometric analysis of histological sections showed an increase in mean percentages of newly osteoid and bone marrow from 6 to 12 weeks. Conversely, it showed a decrease in mean percentage of connective tissue from 6 to 12 weeks in all the groups.

For intergroup comparison, OPG-chitosan gel group showed the highest mean percentages value in new bone formation (41.02 ± 1.00), osteoid (27.02 ± 0.97) and bone marrow (10.28 ± 1.62) at 6 weeks followed by chitosan gel group. At 12 weeks, group C exhibited the highest mean percentages in new bone formation (55.27 ± 11.10) and bone marrow (15.00 ± 7.00), whereas chitosan gel group showed the highest mean percentages

of osteoid (34.13 ± 1.03). There were no significant results in bone marrow between chitosan gel and OPG-chitosan gel groups ($p = 1.000$) at 12 weeks. Controversially, control group showed significantly ($p = 0.000$) the highest mean percentages of fibrous tissue (98.33 ± 0.58) at both time points (**Table 2**).
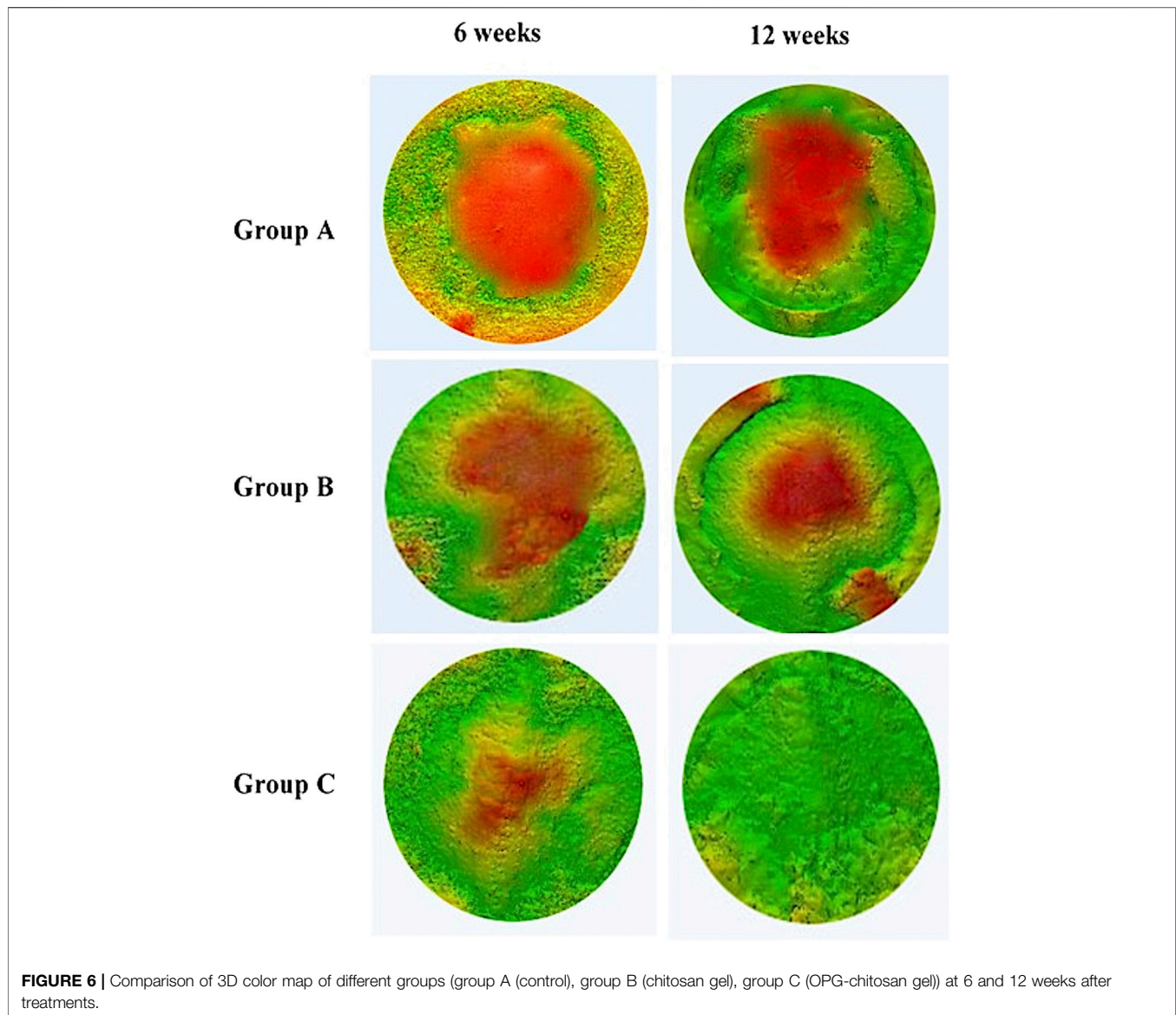
DISCUSSION

The current study aimed to study the characteristics of newly formed bone (microstructure, volume, and density) in the implanted chitosan-based gel scaffolds using HR-pQCT and histomorphometric analysis.

In the present study, rabbit was selected as an experimental model because it is available, simple to house, easy to handle, economical, adequate for the preparation of bone cavities, and suitable model for bone ingrowth and biomaterial studies. Rabbit animal model is considered one of the most used animals for medical research and covers approximately 35% of musculoskeletal research studies (Neyt et al., 1998). Moreover, it is one of the International Standards established regarding the species suitable for testing implantation of materials in bone for reconstruction, fracture or osteotomy, bone in-growth and bone defect repair, and for evaluating the potential application of the material such as the process of material degradation and replacement by host tissue.

The critical size defect (CSD) has been defined as the smallest intraosseous wound in an animal that will not heal spontaneously when left untreated for a certain time period or which shows less than 10% bone regeneration during the lifetime of the animal. It has been shown that the animal calvaria is an accurate and reproducible model for testing bone graft materials as it has many similarities to the maxillofacial region as acceptor site (Isaksson, 1991). Furthermore, the cranial defect does not require fixation as it is supported by dura and the overlying skin as reported by An and Freidman (1998). Rentsch et al., in 2014 created a circular skull defect of 15 mm diameter placed centrally within the parietal bone (Rentsch et al., 2014). Since the clinical outcome of grafting procedure depends on the local and systemic conditions and in agreement with the previous mentioned studies, the authors of this study found that the most suitable area to create a well-defined critical size defect without affect the major anatomic structure in the rabbit cranium was the central part which couldn't be created without involving the sagittal suture. Furthermore, the central part of the cranium has a good size for easier surgical procedure, simple specimen handling, well established reproducibility and less morbidity. Additionally, it is a plate which permits creations of a uniform circular defect that allows appropriate radiographic and histological analysis. Sohn et al. (2010) reported that the other part of cranium could not get more than 11 mm in diameter. Concerning sample size determination, three rabbit in each group were suitable for this study according to sample size formula for animal studies published in 2013 (Charan and Biswas, 2013).

The HR-pQCT is an automated method that could be used to evaluate the trabecular and cortical bone microstructure and has several advantages over manual analysis. This is an agreement

FIGURE 6 | Comparison of 3D color map of different groups (group A (control), group B (chitosan gel), group C (OPG-chitosan gel)) at 6 and 12 weeks after treatments.

with Baiker study, mentioning the automated method of analysis can be purely objective, handle every dataset in the same manner and much faster than any manual procedures (Baiker et al., 2012). In addition, HR-pQCT has been considered a useful and reliable method for evaluating bone healing as shown in previous term studies (Maréchal et al., 2005; Acar et al., 2016). Baek et al. used μCT to evaluate chitosan-based membrane in a rat model and concluded that the membrane had a significant effect on the new bone formation (Baek et al., 2016). It was suggested that the membrane has the potential for guided bone regeneration application. The same finding was observed by Him et al. (He et al., 2015) who evaluated nano-hydroxyapatite-chitosan in a rat model. In the present study, the amount of newly formed bone volume, bone volume densities, and microstructure that were measured using the histomorphometric analysis and HR-pQCT analysis was highly correlated in the newly formed bone in chitosan gel and OPG-chitosan gel implantation sites on

rabbit calvarial defects. This result was similar to Park et al. study who reported that histomorphometric analysis and micro-CT analysis were valid methods for measurement of the new bone (Park et al., 2011).

Chitosan has favorable properties including biocompatibility, biodegradability, antibacterial, and biological activity, as well as its renewable character. Some studies reported that creating a chitosan in hydrogel form would provide a good environment for encapsulation and localized delivery of cells and cell proliferation (Shariatinia and Jalali, 2018; Ahsan et al., 2020). Additionally, the hydrogel would make chitosan respond to various stimuli for example, temperature, heat, light, pH, ionic strength, humidity, and redox potential that are playing an important role for biomedical applications such as drug delivery and tissue engineering (Hu et al., 2017). Aycan and Alemdar in 2018 reported that bone ash-reinforced, pH-sensitive, chitosan-

TABLE 2 | Histomorphometri results demonstrating the mean percentages of new bone formation, osteoid, bone marrow and fibrous tissue in groups (group A (control), group B (chitosan gel), group C (OPG-chitosan gel)) at 6 and 12 weeks.

Bone regeneration	Group A	Group B	Group C
6 weeks			
New bone %	0.67 ± 0.05	11.39 ± 0.79	41.02 ± 1.00
Osteoid %	1.00 ± 0.14	19.10 ± 1.02	27.02 ± 0.97
Bone marrow %	0.00	3.00 ± 0.23	10.28 ± 1.62
Fibrous tissue %	98.33 ± 0.58	64.31 ± 1.34	19.00 ± 1.00
12 weeks			
New bone %	15.01 ± 1.00	25.53 ± 1.50	55.27 ± 11.10
Osteoid %	9.40 ± 1.51	34.13 ± 1.03	29.79 ± 8.58
Bone marrow %	2.33 ± 1.50	9.00 ± 1.00	15.00 ± 7.00
Fibrous tissue %	68.28 ± 8.11	30.03 ± 4.78	5.00 ± 2.04

Significant difference over time based on One-Way ANOVA ($p \leq 0.05$). Significant difference over time based on independent-samples t-test ($p < 0.05$).

based hydrogel could be used as a drug carrier for the controlled release of amoxicillin in the treatment of gastric ulcer. They verified that it would be a good alternative to present biomaterials for the future applications in tissue engineering and regenerative drug systems (Aycan and Alemdar, 2018). In corresponding with previous mentioned studies, all the present investigation was consistent and revealed that the chitosan gel and OPG-chitosan gel demonstrating a significant bone quantity and quality on rabbit calvarial defects compared to unfilled surgical defect. It showed that the density of tissue in the center of the chitosan filled defects was much higher than the density of soft tissue in the unfilled defects in both time points (6 and 12 weeks). This indicated earlier woven and lamellar bone formation subsequently in chitosan filled defects, which could establish and maintain defect healing in a dynamic process in chitosan's' groups, than those occurred in unfiled defects. In terms of bone quantity, the histomorphometric result showed that the chitosan gel group showed higher bone mean percentage than the control group by 10.52% but less than in OPG-chitosan group by 29.74% at 12 weeks. The author suggests that the superiority of chitosan's groups on bone quantity and quality to control group is related to the cationic nature of chitosan which allow electrostatic interactions with anionic glycosaminoglycans that modulate the action of several cytokines and growth factors. This property is of crucial importance in bone regeneration as reported by Di Martino et al. (2005). While the superiority of OPG-chitosan gel group in bone volume and density compared to other groups at both time points referred to the enhancement of chitosan gel with the OPG protein, which could regulate bone remodeling and osteoclastogenesis (Jayash et al., 2020). This is an agreement with the previous studies that showed an increase in bone mineral density by using recombinant OPG protein in rodents (Capparelli et al., 2003; Graber et al., 2016).

Chitosan has been described as a potent wound-healing accelerator (Di Martino et al., 2005). In the present study, 3D models of surgical sites showed major differences between reference bone and the newly formed bone tissues after 6 and 12 weeks in the control group, whereas it was comparable to chitosan's' groups. This could verify that all parts of the defects in chitosan's' groups were filled with thicker trabecular new bone than that in unfilled defects. Moreover, the chitosan gel enables the defect to heal more rapidly than an empty, unfilled defect, which was filled with just osteoid tissue at 6 weeks. The authors suggested that the earlier and more bone formed in chitosan gel and OPG-chitosan gel filled defects were resulted from the action of the hydrophilic surface of chitosan gel that promotes cell adhesion and supports the attachment and proliferation of bone-forming osteoblast cells as well as formation of a mineralized bone matrix. Additionally, as a result of the advantage of hydrogels in chitosan that can easily adopt the geometry of the defect that they occupy which has a role in stability that supports the cell differentiation and proliferation as reported by Levengood and Zhang (2014).

In a bony defect, the most intense cellular reaction occurs during the first 6 weeks. In another word, the defect is first bridged by a trabecular framework consisting of primitive woven bone. Following, there is a reduction in the numbers of cells in these areas, as well as an increase in calcium deposition as reported by Gehrke (2013). The quantity of osteoblasts is significantly changed, and the bone remodeling occur between 30 and 45 days (Piattelli et al., 1995). Moreover, the defect closure and the new bone area ratio gradually increased with the healing time, but these parameters did not differ significantly between weeks 2 and 4 or between weeks 8 and 12 (Sohn et al., 2010). An observation period of at least 12 weeks was recommended by Bodde et al. (2008). Furthermore, Seo and Kim (2020) stated that the volume analysis of rabbit calvarial defects and bone grafts using CT can be done after 2 and 8 weeks. In point of fact, the HR-pQCT results were corresponding to the histological results of our published literature in 2007 (Jayash et al., 2017a; Jayash et al., 2017b). Likewise, in the current study, the part-comparison map and histomorphometrical analyses results confirmed the changes in microstructure between the reference bone and the newly formed bone after surgery at 6 and 12 weeks. They showed that the rate of the bone healing was higher in the OPG-chitosan gel and chitosan gel than in the unfilled defect. Furthermore, the defects healed completely at 12 weeks in the OPG-chitosan gel implanted defects and partially, more prominent at chitosan gel than the control defects. Although both control and chitosan gel groups both exhibited partially defects closure at 12 weeks, chitosan gel group showed higher mean percentages of osteoid with no significant results in bone marrow with OPG-chitosan gel group at 12 weeks which indicated more newly formed bone quantity in chitosan gel than the control group. This is an evidence of the ability of chitosan gel to play a supportive role in the early repair process and provides a favorable surface for osteoprogenitor cell attachment.

To sum up, the chitosan gel was capable of regenerating new bone which is beneficial in tissue engineering applications, and the HR-pQCT analysis was an efficient method to evaluate the newly formed bone and it was as effective as the histomorphometry bone analysis. Potentially, these findings could be translated into clinical use and would be of great interest to the vision scientists, researchers, clinicians, and trainees.

CONCLUSION

The chitosan-based gel promoted the cell migration, proliferation, and differentiation in support of tissue regeneration by demonstrating a significant bone quantity and quality in a cranial critical size defect in a rabbit model compared to unfilled surgical defect. Correspondingly, the OPG enhanced the chitosan gel in bone regeneration. This study has revealed that chitosan-based gel is potential candidates for bone tissue engineering.

DATA AVAILABILITY STATEMENT

The original contributions presented in the study are included in the article/Supplementary Material, further inquiries can be directed to the corresponding authors.

ETHICS STATEMENT

The animal study was reviewed and approved by Institutional Animal Care and Use Committee (FOM IACUC).

AUTHOR CONTRIBUTIONS

SJ conceived and designed the experiments, performed the experiments, analyzed the data, wrote the paper, prepared figures and/or tables, reviewed drafts of the paper. NH, MM, and NB conceived and designed the experiments, contributed in reagents/materials/analysis tools, reviewed drafts of the paper. NA-N and NI reviewed drafts of the paper and contributed in analysis tools.

FUNDING

ACKNOWLEDGMENTS

REFERENCES

Acar, A. H., Yolcu, Ü., Altındiş, S., Gül, M., Alan, H., and Malkoç, S. (2016). Bone regeneration by low-level laser therapy and low-intensity pulsed ultrasound therapy in the rabbit calvarium. *Arch. Oral Biol.* 61, 60–65. doi:10.1016/j.archoralbio.2015.10.011

Ahsan, A., Farooq, M. A., and Parveen, A. (2020). Thermosensitive chitosan-based injectable hydrogel as an efficient anticancer drug carrier. *ACS omega* 5, 20450–20460. doi:10.1021/acsomega.0c02548

Al-Namnam, N., and Jayash, S. N. (2019). Recent advances in bone graft substitute for oral and maxillofacial applications:A review. *Int. J. Biosci.* 15, 70–94. doi:10.12692/ijb/15.4.70-94

Alyessary, A. S., Yap, A. U. J., Othman, S. A., Rahman, M. T., and Radzi, Z. (2017). Effect of piezoelectric sutural ostectomies on accelerated bone-borne sutural expansion. *J. Oral Maxillofac. Surg.* 76, 616–630. doi:10.1016/j.joms.2017.08.018

An, Y. H., and Freidman, R. J. (1998). *Animal models in orthopaedic research*. Boca Rato, FL; CRC Press .

Aycan, D., and Alemdar, N. (2018). Development of pH-responsive chitosan-based hydrogel modified with bone ash for controlled release of amoxicillin. *Carbohydr. Polym.* 184, 401–407. doi:10.1016/j.carbpol.2017.12.023

Baek, Y. J., Kim, J. H., Song, J. M., Yoon, S. Y., Kim, H. S., and Shin, S. H. (2016). Chitin-fibroin-hydroxyapatite membrane for guided bone regeneration: micro-computed tomography evaluation in a rat model. *Maxillofac. Plast. Reconstr. Surg.* 38, 14. doi:10.1186/s40902-016-0060-6

Baiker, M., Snoeks, T. J., Kaijzel, E. L., Que, I., Dijkstra, J., Lelieveldt, B. P., et al. (2012). Automated bone volume and thickness measurements in small animal whole-body microCT data. *Mol. Imaging Biol.* 14, 420–430. doi:10.1007/s11307-011-0522-2

Bodde, E. W., Spauwen, P. H., Mikos, A. G., and Jansen, J. A. (2008). Closing capacity of segmental radius defects in rabbits. *J. Biomed. Mater. Res. A.*, 85, 206–217. doi:10.1002/jbm.a.31549

Bumgardner, J., Wiser, R., Elder, S., Jouett, R., Yang, Y., and Ong, J. (2003). Contact angle, protein adsorption and osteoblast precursor cell attachment to chitosan coatings bonded to titanium. *J. Biomater. Sci. Polym. Ed.* 14, 1401–1409. doi:10.1163/156856203322599734

Capparelli, C., Morony, S., Warmington, K., Adamu, S., Lacey, D., Dunstan, C. R., et al. (2003). Sustained antiresorptive effects after a single treatment with human recombinant osteoprotegerin (OPG): a pharmacodynamic and pharmacokinetic analysis in rats. *J. Bone Miner Res.* 18, 852. doi:10.1359/jbmr.2003.18.5.852

Chang, H. H., Wang, Y. L., Chiang, Y. C., Chen, Y. L., Chuang, Y. H., Tsai, S. J., et al. (2014). A novel chitosan-γPGA polyelectrolyte complex hydrogel promotes early new bone formation in the alveolar socket following tooth extraction. *PLoS one* 9, e92362. doi:10.1371/journal.pone.0092362

Charan, J., and Biswas, T. (2013). How to calculate sample size for different study designs in medical research? *Indian J. Psychol. Med.* 35 (2), 121. doi:10.4103/0253-7176.116232

Di Martino, A., Sittinger, M., and Risbud, M. V. (2005). Chitosan: a versatile biopolymer for orthopaedic tissue-engineering. *Biomaterials* 26, 5983–5990. doi:10.1016/j.biomaterials.2005.03.016

Gehrke, S. A. (2013). Analysis of bone tissue healing around titanium implant surface treated with tio sandblasted after three and six weeks used different histological methods-a study in rabbits. *Sci. J. Med. Clin. Trials* 2013, 1–7. doi:10.7237/sjmct/150

Graber, L. W., Vanarsdall, R. L., Jr, Vig, K. W., and Huang, G. J. (2016). *Orthodontics: Current principles and techniques*. New York, NY: Elsevier Health Sciences.

He, Y., Dong, Y., Cui, F., Chen, X., and Lin, R. (2015). Ectopic osteogenesis and scaffold biodegradation of nano-hydroxyapatite-chitosan in a rat model. *PLoS one* 10, e0135366. doi:10.1371/journal.pone.0135366

Hu, J., Chen, Y., Li, Y., Zhou, Z., and Cheng, Y. (2017). A thermo-degradable hydrogel with light-tunable degradation and drug release. *Biomaterials* 112, 133–140. doi:10.1016/j.biomaterials.2016.10.015

Isaksson, S. (1991). Aspects of bone healing and bone substitute incorporation. An experimental study in rabbit skull bone defects. *Swed Dent J. Suppl.* 84, 1–46.

Jayash, S. N., Hashim, N. M., Misran, M., and Baharuddin, N. (2017a). Formulation and *in vitro* and *in vivo* evaluation of a new osteoprotegerin-chitosan gel for bone tissue regeneration. *J. Biomed. Mater. Res. A.* 105, 398–407. doi:10.1002/jbm.a.35919

Jayash, S. N., Hashim, N. M., Misran, M., and Baharuddin, N. (2016). *In vitro* evaluation of osteoprotegerin in chitosan for potential bone defect applications. *PeerJ.* 4, e2229. doi:10.7717/peerj.2229

Jayash, S. N., Hashim, N. M., Misran, M., and Baharuddin, N. (2017b). Local application of osteoprotegerin-chitosan gel in critical-sized defects in a rabbit model. *PeerJ.* 5, e3513. doi:10.7717/peerj.3513

Jayash, S. N., Al-Namnam, N. M., and Shaghayegh, G. (2020). Osteoprotegerin (OPG) pathways in bone diseases and its application in therapeutic

perspectives. *Biointerface Res. Appl. Chem.* 10, 5913–5200. doi:10.33263/BRIAC102.193200

Lee, J. H. (2018). Injectable hydrogels delivering therapeutic agents for disease treatment and tissue engineering. *Biomater. Res.* 22, 1–14. doi:10.1186/s40824-018-0138-6

Levengood, S. L., and Zhang, M. (2014). Chitosan-based scaffolds for bone tissue engineering. *J. Mater. Chem. B Mater. Biol. Med.* 2, 3161–3184. doi:10.1039/C4TB00027G

Malviya, R. (2020). Exploration of neem gum-chitosan and kheri gum-chitosan polyelectrolyte complex-based film for transdermal delivery of protein/peptideBiointerface. *Biointerface Res. Appl. Chem.* 10, 5860–5868. doi:10.2174/2210315509666190515112704

Maréchal, M., Luyten, F., Nijs, J., Postnov, A., Schepers, E., and van Steenberghe, D. (2005). Histomorphometry and micro-computed tomography of bone augmentation under a titanium membrane. *Clin. Oral Implants Res.* 16, 708–714. doi:10.1111/j.1600-0501.2005.01205.x

Neyt, J., Buckwalter, J. A., and Carroll, N. (1998). Use of animal models in musculoskeletal research. *Iowa Orthop. J.* 118, 118–123.

Park, S. Y., Kim, K. H., Koo, K. T., Lee, K. W., Lee, Y. M., Chung, C. P., et al. (2011). The evaluation of the correlation between histomorphometric analysis and micro-computed tomography analysis in AdBMP-2 induced bone regeneration in rat calvarial defects. *J. Periodontal Implant Sci.* 41, 218–226. doi:10.5051/jpis.2011.41.5.218

Particelli, F., Mecozzi, L., Beraudi, A., Montesi, M., Baruffaldi, F., and Viceconti, M. (2012). A comparison between micro-CT and histology for the evaluation of cortical bone: Effect of polymethylmethacrylate embedding on structural parameters. *J. Microsc.* 245, 302–310. doi:10.1111/j.1365-2818.2011.03573.x

Piattelli, A., Scarano, A., and Piattelli, M. (1995). Detection of alkaline and acid phosphatases around titanium implants: a light microscopical and histochemical study in rabbits. *Biomaterials* 16, 1333–1338. doi:10.1016/0142-9612(95)91049-5

Rentsch, C., Rentsch, B., Heinemann, S., Bernhardt, R., Bischoff, B., Förster, Y., et al. (2014). ECM inspired coating of embroidered 3D scaffolds enhances calvaria bone regeneration. *Biomed. Res. Int.* 2014, 217078. doi:10.1155/2014/217078

Seo, S. J., and Kim, Y. G. (2020). Improved bone regeneration using collagen-coated biphasic calcium phosphate with high porosity in a rabbit calvarial model. *Biomed. Mater.* 16, 015012. doi:10.1088/1748-605x/abb1fc

Shariatinia, Z., and Jalali, A. M. (2018). Chitosan-based hydrogels: Preparation, properties and applications. *Int. J. Biol. Macromol.* 115, 194–220. doi:10.1016/j.ijbiomac.2018.04.034

Sharma, A., and Sharma, P. K. (2020). Stimuli-responsive supramolecules for bone tissue engineering. *Biointerface Res. Appl. Chem.* 10, 5122–5127. doi:10.33263/BRIAC102.122127

Sohn, J. Y., Park, J. C., Um, Y. J., Jung, U. W., Kim, C. S., Cho, K. S., et al. (2010). Spontaneous healing capacity of rabbit cranial defects of various sizes. *J. Periodontal Implant Sci.* 40, 180–187. doi:10.5051/jpis.2010.40.4.180